Optics Letters

Parity–time-symmetric frequency-tunable optoelectronic oscillator with a single dual-polarization optical loop

PENG LI,[1,2] ZHENG DAI,[1] ZHIQIANG FAN,[1] LIANSHAN YAN,[2] AND JIANPING YAO[1,*]

[1]Microwave Photonics Research Laboratory, School of Electrical Engineering and Computer Science, University of Ottawa, Ottawa, Ontario K1N 6N5, Canada
[2]Center for Information Photonics and Communications, School of Information Science and Technology, Southwest Jiaotong University, Chengdu 611756, China
*Corresponding author: jpyao@uottawa.ca

Received 8 April 2020; revised 2 May 2020; accepted 3 May 2020; posted 4 May 2020 (Doc. ID 394719); published 1 June 2020

We propose and experimentally demonstrate a parity–time (PT)-symmetric frequency-tunable optoelectronic oscillator (OEO) in which the PT symmetry is implemented based on a single dual-polarization optical loop. By employing the inherent birefringence of a z-cut lithium niobate ($LiNbO_3$) phase modulator (PM), two mutually coupled optoelectronic loops supporting orthogonally polarized light waves with one experiencing a gain and the other a loss are implemented. By controlling the gain, loss, and the coupling coefficients between the two loops, the PT symmetry breaking condition is met, which enables the OEO to operate in single mode without using an ultranarrow passband optical or microwave filter. The frequency tunability is realized using a microwave photonic filter (MPF) implemented using the PM and a phase-shifted fiber Bragg grating (PS-FBG). The proposed PT-symmetric OEO is experimentally evaluated. A stable and frequency-tunable microwave signal from 2 to 12 GHz is generated. The phase noise of the generated signal at 11.8 GHz is measured, which is −124 dBc/Hz at a frequency offset of 10 kHz.

https://doi.org/10.1364/OL.394719

An optoelectronic oscillator (OEO) is a hybrid microwave and photonic system with an amplified optoelectronic feedback loop. An OEO can be used to generate a high-frequency and low phase noise microwave signal, which can find applications such as wireless communications, radar, and electronic warfare [1–3]. The phase noise performance of an OEO is associated with the length of the optoelectronic feedback loop. To generate a high-quality microwave signal with a low phase noise, a long feedback loop is needed. In Ref. [4], a 10 GHz microwave signal with a phase noise as low as −163 dBc/Hz at a frequency offset of 6 kHz was generated by an OEO with a feedback loop of 16 km. However, an OEO with a long feedback loop will have a large number of closely spaced longitudinal modes due to its small free spectral range (FSR), which makes it difficult to select a single mode to achieve single-mode oscillation. In general, to select a single mode, an ultranarrow passband optical or microwave filter is needed, but an ultranarrow passband filter is hard to implement. For the past few years, numerous methods have been reported to implement widely frequency-tunable OEOs based on a tunable microwave bandpass filter [5], or a microwave photonic filter (MPF) [6–9]. Since the bandwidths of the filters reported in [5–9] are still wide, the loop length cannot be long; thus, the phase noise is still high. A solution to the problem is to use a dual- or multiple-loop OEO. Based on the Vernier effect, the effective FSR can be increased, which makes the selection of a single mode easier [10,11]. However, an OEO using dual or multiple loops will make its frequency tunability limited, or the lengths of the loops must be controlled when performing frequency tuning, which makes the implementation complicated. In addition, the use of dual or multiple loops can deteriorate the stability of the OEO.

Recently, a new concept, parity–time (PT) symmetry, has been introduced and employed for mode selection in optical and microwave systems, such as fiber or integrated lasers [12–14], purely electronic microwave oscillators [15], and OEOs [16,17]. In a PT-symmetric OEO, for example, single mode selection can be effectively achieved based on PT symmetry without using an ultranarrow passband filter. In the implementation of a PT-symmetric OEO, two mutually coupled feedback loops that are identical in geometry, but with one having a gain and the other a loss, are needed. When the gain and loss coefficients are identical in magnitude, and are larger than the coupling coefficient, PT symmetry is broken, one single mode is selected, and other modes are suppressed. We have recently demonstrated this concept in an OEO in which a microwave signal at 9.8 GHz with a phase noise of −142.5 dBc/Hz at an offset frequency of 10 kHz was generated [16]. A similar approach was also reported in which a microwave signal at ∼4 GHz with a phase noise of −139 dBc/Hz was generated [17]. The limitation of the approaches in Refs. [16,17] is that PT symmetry in the OEOs was achieved using two physically separated loops, making the implementation complicated and the stability poor. In addition, the frequency of the generated microwave signal was fixed. For many applications, frequency tuning over a large frequency range is highly needed. A frequency-tunable PT-symmetric OEO was reported [18]. Again, two physically separated feedback loops were employed. Recently, we proposed a frequency-tunable PT-symmetric OEO having a single physical loop [19]. The key limitation of the approach is that multiple polarization controllers (PCs) are used to control the gain, loss and coupling coefficients, making the implementation complicated.

In this Letter, we propose and experimentally demonstrate a PT-symmetric frequency-tunable OEO based on a single dual-polarization optical loop. By employing the inherent birefringence of a z-cut lithium niobate ($LiNbO_3$) phase modulator (PM), two mutually coupled optoelectronic loops supporting orthogonally polarized light waves with one having a gain and the other a loss are implemented. By controlling the gain, loss, and coupling coefficient between the two feedback loops, the PT symmetry breaking condition is met, which enables the OEO to operate in single mode without using an ultranarrow passband optical or microwave filter. The coarse frequency selection is realized by a MPF implemented using the PM and a phase-shifted fiber Bragg grating (PS-FBG). By tuning the wavelength spacing between the optical carrier and the notch of the PS-FBG filter, the center frequency of the MPF is tuned, and the oscillation frequency is tuned. The approach is experimentally demonstrated. A stable and frequency-tunable microwave signal from 2 to 12 GHz is generated. The phase noise of the generated signal at 11.8 GHz is measured to be −124 dBc/Hz at a frequency offset of 10 kHz.

$LiNbO_3$ crystal is a negative uniaxial material with the ordinary refractive index greater than the extraordinary refractive index, which has been widely used in integrated and guided-wave optics, due to its inherent advantages in terms of excellent electro-optic, acousto-optic, and piezoelectric properties [20,21]. For a z-cut $LiNbO_3$ PM, both the ordinary and extraordinary optical modes are supported, but with different modulation efficiencies, as shown in Fig. 1(a). Assume an optical carrier with a power of P that is linearly polarized with a polarization angle of θ with respect to the z axis is sent to a z-cut PM, to which an external electrical signal $s(t)$ is applied, to modulate the light components along the horizontal and vertical axes of the PM. The modulated optical signals at the output of the PM can be expressed as

$$\begin{bmatrix} E_x \\ E_z \end{bmatrix} = \sqrt{P} \begin{bmatrix} \sin\theta \exp j\left(\frac{s(t)\pi}{V_\pi^{TE}}\right) \\ \cos\theta \exp j\left(\frac{s(t)\pi}{V_\pi^{TM}}\right) \end{bmatrix}, \quad (1)$$

where V_π^{TE} and V_π^{TM} are the half-wave voltages of the PM for the TE and TM modes, respectively. For the $LiNbO_3$ PM, the ratio between V_π^{TE} and V_π^{TM} is ∼3 [22]. It can be seen from Eq. (1) that the optical power splitting ratio between the two orthogonally polarized optical signals can be arbitrarily tuned by controlling the polarization angle θ. Based on the above theory, a single-loop dual-polarization PT-symmetric OEO is proposed, with the configuration shown in Fig. 1(b). It consists of a laser diode (LD), a PC, a z-cut $LiNbO_3$ PM, a single-mode fiber (SMF), an optical circulator, a PS-FBG, an erbium-doped fiber amplifier (EDFA), a photodetector (PD), an electrical amplifier (EA), and an electrical divider (ED). A linearly polarized light wave from the LD is sent into the z-cut PM via the PC. By tuning the PC, the polarization angle θ can be tuned. At the output of the PM, two orthogonally polarized optical

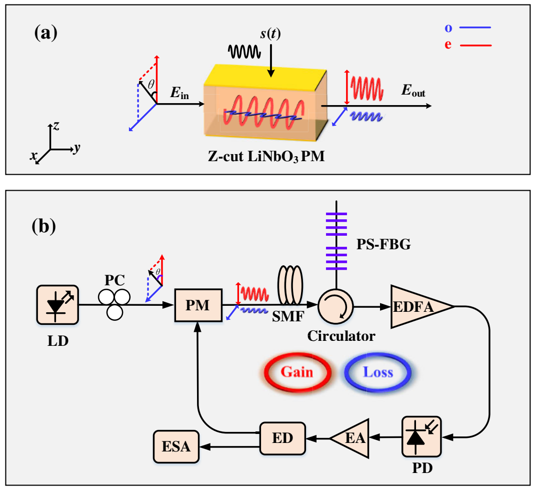

Fig. 1. (a) z-cut $LiNbO_3$ phase modulator that supports both ordinary and extraordinary optical modes; and (b) schematic diagram of the proposed single-loop frequency-tunable PT-symmetric OEO. LD, laser diode; PC, polarization controller; SMF, single-mode fiber; PS-FBG, phase-shifted fiber Bragg grating; EDFA, erbium-doped fiber amplifier; PD, photodetector; EA, electrical amplifier; ED, electrical divider; ESA, electrical spectrum analyzer.

signals that are modulated with different modulation depths are generated. Note that the power splitting ratio between the two orthogonally polarized signals is dependent on the polarization angle θ. After transmission over the SMF, the optical signals are sent to the PS-FBG via the optical circulator. The PS-FBG is used as an optical notch filter to filter out one sideband of the phase-modulated signals to achieve phase modulation to intensity modulation (PM–IM) conversion [23]. The joint operation of the tunable LD, the PM, the PS-FBG, and the PD corresponds to a tunable MPF [23]. The filtered optical signals are amplified by the EDFA and then detected at the PD. The detected electrical signals are amplified by the EA and then divided into two parts by a 3 dB electrical power divider, with one part fed back to the PM to close the OEO loop, and the other sent to the electrical spectrum analyzer (ESA) for spectrum measurements. In the proposed single-loop dual-polarization OEO, the TE and TM modes are confined in the same physical loop, and the power splitting ratio is tunable, which enables the two mutually coupled loops to be controlled with one having a gain and the other a loss. When the gain and the loss coefficients are equal in magnitude, and the gain/loss is greater than the coupling coefficient, PT-symmetric is broken, and single-mode oscillation is enabled. The frequency tunability of the OEO is implemented by tuning the central frequency of the MPF.

In the proposed PT-symmetric OEO, the interplay between the nth longitudinal modes can be expressed as [14]

$$\frac{d}{dt}\begin{bmatrix} G_n \\ L_n \end{bmatrix} = \begin{bmatrix} g_n - j\omega_n, & jk \\ jk, & l_n - j\omega_n \end{bmatrix} \begin{bmatrix} G_n \\ L_n \end{bmatrix}, \quad (2)$$

where ω_n is the angular frequency of the nth mode; g_n and l_n are the net gain coefficients of the nth modes in the gain and loss loops, respectively; and k is the coupling coefficient between the two loops. According to Eq. (2), the eigenfrequencies of the proposed system are given by

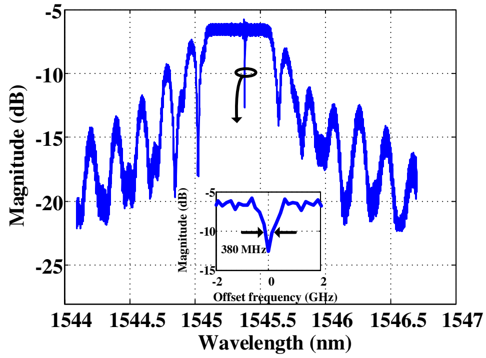

Fig. 2. Measured magnitude spectral response of the PS-FBG in reflection. The inset gives a zoom-in view of the notch of the PS-FBG.

$$\omega_n{}^{(1,2)} = \omega_n + j\frac{g+l}{2} \pm \sqrt{k^2 - \left(\frac{g-l}{2}\right)^2}. \quad (3)$$

Under the PT symmetry condition, the gain and loss are equal in magnitude, and Eq. (3) can be simplified as

$$\omega_n{}^{(1,2)} = \omega_n \pm \sqrt{k^2 - g^2}. \quad (4)$$

It can be seen from Eq. (4) that, when the gain/loss coefficient is less than the coupling coefficient, two frequencies will be generated, which indicates that PT symmetry is unbroken. However, when the gain/loss coefficient is greater than the coupling coefficient, a pair of conjugate complex amplifying and decaying modes will emerge, which indicates PT symmetry is broken, and single-mode oscillation will be achieved.

To verify the proposed PT-symmetric OEO, an experiment is performed based on the setup shown in Fig. 1(b). A light wave with an optical power of 9 dBm generated from the LD (Yokogawa, AQ2201) is sent to the z-cut PM via the PC. The PM (LN66S-FC) has a 3 dB bandwidth of 40 GHz and an insertion loss of 4 dB. The key device in the system is the PM. Since no internal polarizer is incorporated in the PM, the PM can support both ordinary and extraordinary modes. The PC (JDS Uniphase, PR2000) is an electrically controlled device consisting of a polarizer, a quarter-wave retarder, and a half-wave retarder, which is used to adjust the state of polarization (SOP) of the light wave entering the PM. After transmission over the SMF of a length of 5 km, the optical signal is filtered by the PS-FBG and then amplified by the EDFA with a fixed output optical power of 0 dBm. The magnitude response of the PS-FBG is shown in Fig. 2, which is measured using an optical vector analyzer (OVA, LUNA 5000) with a resolution of 1.6 pm. The full width at half-maximum (FWHM) of the PS-FBG is about 380 MHz, as shown in the inset in Fig. 2. The amplified optical signal is converted to an electrical signal at the PD. Then, the electrical signal is amplified by two cascaded EAs (Multilink Tech Corp, MTC5515-751) to provide a sufficiently high gain. Finally, the electrical signal is fed back to the PM to close the loop. Part of the electrical signal is taped by the ED with its electrical spectrum monitored by the ESA (Agilent E4448A). The phase noise of the electrical signal is measured by a signal analyzer (Agilent E5052B) together with a downconverter (Agilent E5053A). The downconverter is used to extend the highest measurement frequency from 7 to 26.5 GHz.

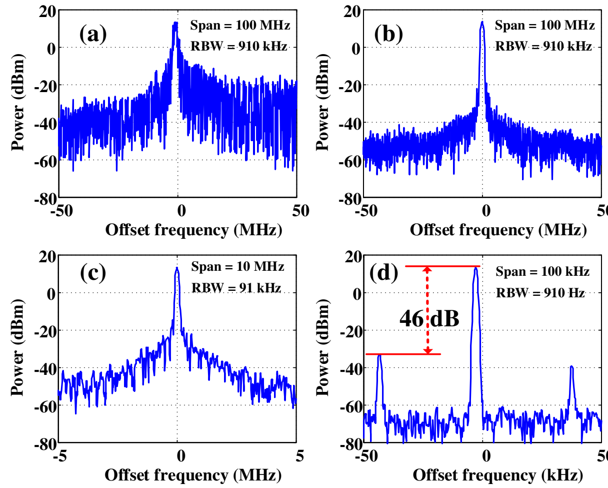

Fig. 3. Electrical spectra of the generated microwave signals at a central frequency of 11.8 GHz. (a) Multimode oscillation measured with a span of 100 MHz and an RBW of 910 kHz; (b) single-mode oscillation measured with a span of 100 MHz and an RBW of 910 kHz; (c) single-mode oscillation measured with a span of 10 MHz and an RBW of 91 kHz; and (d) single-mode oscillation measured with a span of 100 kHz and an RBW of 910 Hz.

Figure 3 shows the measured electrical spectra of the generated microwave signals at 11.8 GHz. Without PT symmetry, since the MPF has a FWHM of 380 MHz, which is much wider than the FSR of the OEO loop, multimode oscillation resulted, as shown in Fig. 3(a). Note that the electrical spectrum is measured with a span of 100 MHz and a resolution bandwidth (RBW) of 910 kHz. Then, the OEO is reconfigured to operate under the PT symmetry broken condition, which is done by tuning the PC to match the gain and loss coefficients. Note that the coupling coefficient is fixed, since the feedback microwave signal to the PM is equally applied to the light components along the horizontal and vertical axes of the PM, making the coupling ratio 1:1. The loop gain and loss coefficients are controlled to be greater than the coupling coefficient by tuning the loop gain; thus single-mode oscillation is realized. Figures 3(b)–3(d) show the electrical spectra of the generated microwave signal measured with different spans and RBWs. It can be seen that a single-frequency microwave signal is generated, which is measured by the ESA using the same span and RBW with the ones in Fig. 3(a). Figure 3(c) is a zoom-in view of the spectrum in Fig. 3(b), where the span is 10 MHz. Figure 3(d) shows the measured spectrum when the span is set at 100 kHz and the RBW set at 9.1 kHz. Side modes are observed. The mode spacing is 40 kHz, which is identical to the FSR of the OEO loop. The side-mode suppression ratio (SMSR) is 46 dB. Compared with other reported approaches, the proposed approach has a better side SMDR, as shown in Table 1.

The phase noise of the generated single-frequency microwave signal is also measured. As can be seen from Fig. 4, the phase noise is about −124 dBc/Hz at an offset frequency of 10 kHz. Side modes are lower than −63 dBc/Hz, which verifies the effectiveness of using PT symmetry to achieve single-frequency oscillation without the need of an ultranarrow passband optical or microwave filter.

Finally, the frequency tunability of the generated microwave signals is demonstrated. The coarse frequency selection and

Table 1. SMDRs of PT-Symmetric OEOs

Refs.	SMDR (dB)
[16]	26.4
[17]	~30
[18]	40
[19]	45
This work	46

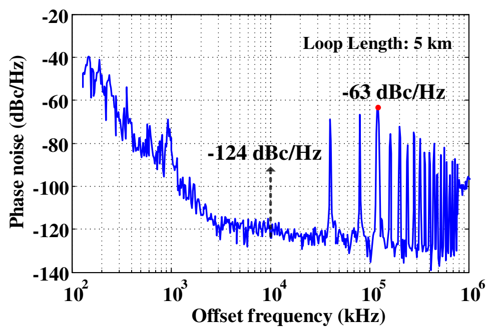

Fig. 4. Phase noise of the generated microwave signal at 11.8 GHz.

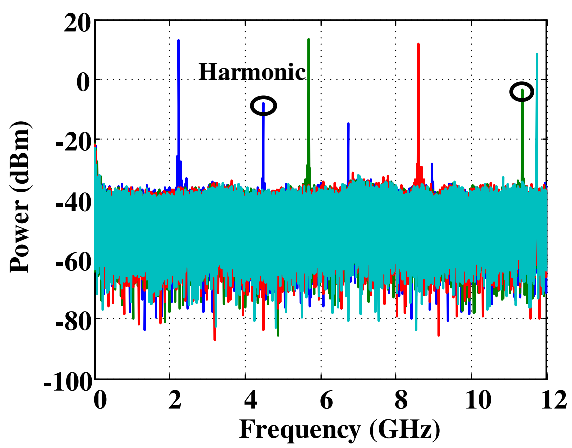

Fig. 5. Frequency tunability of the proposed PT-symmetric OEO.

frequency tuning are performed by tuning the MFP, which is implemented based on the PM and the PM–IM conversion in the PS-FBG. The central frequency of the MFP is equal to the wavelength spacing between the wavelength of the optical wave from the LD and that of the notch of the PS-FBG. In the experiment, the frequency is tuned by tuning the wavelength of the LD. As shown in Fig. 5, the frequency of the OEO is tuned from 2 to 12 GHz. A wider frequency tunable range can be realized if wider bandwidths PM, PD, and EA are employed. Note that the lines marked with circles are the second harmonics of the fundamental microwave signals at 2.1 GHz and 5.6 GHz, generated due to the nonlinearity of the OEO loop.

In summary, we proposed and experimentally demonstrated a single-loop dual-polarization PT-symmetric OEO. The key novelty of this approach compared with the approaches reported in Refs. [18,19] is that only a single PC is needed to control the gain, loss, and coupling coefficients, making the implementation greatly simplified and the stability highly improved.

The key device in the implementation was a PM, which supports two orthogonally polarized modes. By controlling the polarization angle of the light wave into the PM, two equivalent mutually coupled loops with one having a gain and the other a loss were achieved, making the OEO to be PT-symmetric. The frequency tunability of the OEO was realized by using an MPF, which was realized based on PM and PM–PM conversion in a PS-FBG. The proposed PT-symmetric OEO was experimentally demonstrated. A microwave signal with a frequency tuning range from 2 to 12 GHz was generated. The phase noise at 11.8 GHz was measured, which was −124 dBc/Hz at the frequency offset of 10 kHz. The phase noise performance can be further improved if a longer SMF is employed.

Funding. Natural Sciences and Engineering Research Council of Canada.

Acknowledgment. P. Li acknowledges a scholarship from the China Scholarship Council (CSC).

Disclosures. The authors declare no conflicts of interest.

REFERENCES

1. X. Yao and L. Maleki, J. Opt. Soc. Am. B **13**, 1725 (1996).
2. J. Yao, J. Lightwave Technol. **35**, 3489 (2017).
3. L. Maleki, Nat. Photonics **5**, 728 (2011).
4. D. Eliyahu, D. Seidel, and L. Maleki, in *IEEE International Frequency Control Symposium* (2008), pp. 811–814.
5. D. Eliyahu and L. Maleki, in *IEEE MTT-S International Microwave Symposium Digest* (2003), pp. 2185–2187.
6. H. Tang, Y. Yu, Z. Wang, L. Xu, and X. Zhang, Opt. Lett. **43**, 2328 (2018).
7. W. Zhang and J. Yao, J. Lightwave Technol. **36**, 4655 (2018).
8. Z. Fan, Q. Qiu, J. Su, and T. Zhang, Opt. Lett. **44**, 534 (2019).
9. M. Fleyer, A. Sherman, M. Horowitz, and M. Namer, Opt. Lett. **41**, 1993 (2016).
10. X. Yao and L. Maleki, IEEE J. Quantum Electron. **36**, 79 (2000).
11. E. Shumakher and G. Eisenstein, IEEE Photon. Technol. Lett. **20**, 1881 (2008).
12. H. Hodaei, M. Miri, M. Heinrich, D. Christodoulides, and M. Khajavikhan, Science **346**, 975 (2014).
13. L. Feng, Z. J. Wong, R. M. Ma, Y. Wang, and X. Zhang, Science **346**, 972 (2014).
14. W. Liu, M. Li, R. Guzzon, E. Norberg, J. Parker, M. Lu, L. Goldren, and J. Yao, Nat. Commun. **8**, 15389 (2017).
15. J. Schindler, A. Li, M. Zheng, F. Ellis, and T. Kottos, Phys. Rev. A **84**, 040101 (2011).
16. J. Zhang and J. Yao, Sci. Adv. **4**, eaar6782 (2018).
17. Y. Liu, T. Hao, W. Li, J. Capmany, N. Zhu, and M. Li, Light Sci. Appl. **7**, 1 (2018).
18. C. Teng, X. Zou, P. Li, W. Pan, and L. Yan, International Topical Meeting on Microwave Photonics (MWP), Ottawa, Ontario, Canada, October, 2019, paper We4.4.
19. Z. Dai, Z. Fan, C. Li, and J. Yao, Optical Fiber Communications Conference and Exhibition (OFC), San Diego, California, USA, March, 2020, paper Th1C.3.
20. L. Arizmendi, Phys. Status Solidi **201**, 253 (2004).
21. R. S. Weis and T. K. Gaylord, Appl. Phys. A **37**, 191 (1985).
22. B. Haas and T. Murphy, IEEE Photon. Technol. Lett. **19**, 729 (2007).
23. W. Li and J. Yao, IEEE Trans. Microwave Theory Tech. **60**, 1735 (2012).